

Electronic Supporting Information

***In-situ* Fe₂N@N-doped porous carbon hybrids as superior catalysts for oxygen reduction reaction**

Xiaoxiao Huang,^a Ziyu Yang,^a Bing Dong,^a Yazhou Wang,^{a,b} Tianyu Tang^a and Yanglong Hou*^a

^aBIC-EAST, Department of Materials Science and Engineering, College of Engineering, Peking University, Beijing 100871, China. E-mail:

houl@pku.edu.cn.

Experimental Section

Catalyst preparation

Synthesis of HKUST-1: MOFs were prepared as described previously with some modification. ¹ 1 g of 1,3,5-benzenetricarboxylic acid was dissolved in 15 mL N,N-Dimethylformamide and 15 mL anhydrous ethanol. On the other hand, 2.077g of Cu(NO₃)₂·3H₂O was dissolved in 15 mL deionized water. Mix and sonicate the above-mentioned solution for 1 hour and transfer it to a 50 mL vial. The vessel was sealed and heated to 100 °C for 10 hours and then cooled down to room temperature slowly. The blue crystals were filtered out and washed with ethanol for 3 times, and finally dried under vacuum at 120 °C for 8 hours.

Synthesis of porous carbon (PC): The PC was prepared with a pyrolysis and etching process. The prepared HKUST-1 was pyrolyzed at 800 °C for 2 hours under N₂ atmosphere before cooling down to room temperature to get Cu nanoparticles coated with porous carbon marked as Cu@PC. Then the Cu@PC was dispersed in saturated FeCl₃·6H₂O solution and stirred for 24 hours. Then, wash the carbon with DI water for 5 times and dry the product under vacuum at 120 °C for 8 hours.

Synthesis of Fe₂N@NPC: In a typical process, 60 mg PC and 60 mg Iron (II) phthalocyanin (FePc) were dispersed in a 10 mL of ethanol and sonicated for 1 hour to form a uniform solution. It was then dried under vacuum at 120 °C for 8 hours, and then annealed in NH₃ atmosphere at certain temperature for 3 hours. Samples annealed at different temperature were marked as Fe₂N@NPC-x (where the x means the annealing temperature). NPC and annealed FePc were synthesized by a direct annealing process of PC and FePc in ammonia at 500 °C for 3 hours.

Synthesis of Fe₂N@NPC-0.5x and Fe₂N@NPC-2.0x: In a typical process for synthesizing Fe₂N@NPC -0.5x, 60 mg PC and 30 mg FePc were dispersed in a 10 mL of ethanol and sonicated for 1 hour to form a uniform solution. It was then dried under vacuum at 120 °C for 8 hours, and then annealed in NH₃ atmosphere at 500 °C for 3 hours. Fe₂N@NPC -2.0x was synthesized by quadrupling the amount of FePc (120mg), leaving other factors unchanged.

Materials characterization

Powder X-ray diffraction (PXRD) patterns were recorded on a Bruker D8 Advanced diffractometer with Cu K α radiation ($\lambda = 1.5405 \text{ \AA}$). Nitrogen sorption and desorption isotherms were measured using a ASAP 2010 at 77 K. Scanning electron microscopy (SEM), transmission electron microscopy (TEM) and high resolution TEM (HRTEM) images were taken using a Hitachi S-4800 microscope, a FEI Tecnai T20 and a FEI Tecnai F30 microscope, respectively. X-ray photoelectron spectroscopy (XPS) was performed on an Axis Ultra imaging photoelectron spectrometer with the monochromatic Al K α line.

Electrochemical measurements²⁻⁷

The electrochemical measurements were performed on a CHI760E electrochemical workstation using a standard three-electrode system. The catalyst coated glassy carbon rotating disk electrode (RDE, diameter 5 mm) or ring-rotated disk electrode (RRDE, diameter 5 mm), a Pt foil (1 cm \times 1 cm) and an Ag/AgCl electrode with saturated KCl solution were used as a working, counter and reference electrodes respectively. To prepare the working electrode, 2 mg of the as-prepared electrocatalysts or Pt/C (20 wt%

Pt on Vulcan XC-72) was dispersed in 2 mL of ethanol under 1-hour sonication to form a homogeneous ink. Then, 20 μL of the suspension and 5 μL of 0.1 wt% Nafion solution were cast onto the GC electrode in sequence drop by drop and dried in air.

All the electrochemical measurements were carried out at room temperature. Cyclic voltammetry (CV) tests were performed in a N_2 and O_2 -saturated 0.1 M KOH in the potential range of -1.0 V-0.2 V (vs. Ag/AgCl) at a scan rate of 100 mV/s. A rotating disk electrode (RDE) test was conducted at rotating speed from 400 rpm to 1600 rpm in O_2 -saturated 0.1 M KOH. The electron transfer numbers during the oxygen reduction reaction were determined from the Koutechy-Levich equation, which was analysed at different potentials of RED tests. Ring-rotated disk electrode (RRDE) measurement was conducted with the rotating speed fixed at 1600 rpm, and the ring potential was set at 1.2 V versus Ag/AgCl with a scan rate of 50 mV s^{-1} .

$$\frac{1}{J} = \frac{1}{J_L} + \frac{1}{J_K} = \frac{1}{B\omega^{1/2}} + \frac{1}{J_K}$$

$$B = 0.62nFC_0(D_0)^{2/3}\nu^{-1/6}$$

$J_K = nFkC_0$ Here, J represents the measured current density, while J_L and J_K are the diffusion- and kinetic-limiting current densities, respectively. ω is the rotating speed, and n is electron transfer number. F is the Faraday constant (96485 C mol^{-1}), C_0 is the O_2 bulk concentration ($1.26 \times 10^{-6} \text{ mol cm}^{-3}$), D_0 is the O_2 diffusion coefficient in the electrolyte ($1.9 \times 10^{-5} \text{ cm}^2 \text{ s}^{-1}$) and ν is the kinetic viscosity of 0.1 mol L^{-1} KOH ($0.01 \text{ cm}^2 \text{ s}^{-1}$).

The HO_2^- percentage ($\% \text{HO}_2^-$) and the corresponding electron number transferred during the ORR were calculated by the following equations:

$$n = \frac{4I_d}{I_d + I_r/N}$$

$$\% \text{HO}_2^- = 200 \times \frac{I_r/N}{I_d + I_r/N}$$

Here I_d and I_r are the disk current and ring current, respectively. N is the current collection efficiency of the Pt ring (0.37).

Defined information of HKUST-1⁸

HKUST-1 (Hong Kong University of Science and Technology) is an electrically neutral MOF made up of copper nodes and 1, 3, 5-benzenetricarboxylic acid (TMA), whose molecule formula is $[\text{Cu}_3(\text{TMA})_2(\text{H}_2\text{O})_3]_n$. HKUST-1 is composed of cupric tetracarboxylate units, in which the 12 carboxylate oxygens from two TMA ligands bind to four coordination sites for each of the three Cu^{2+} ions.

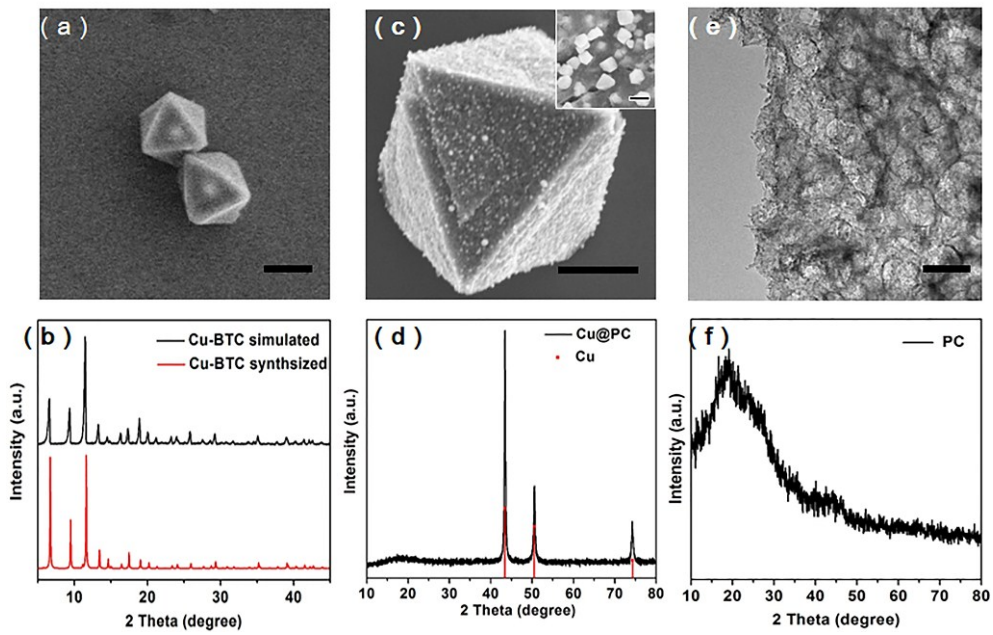
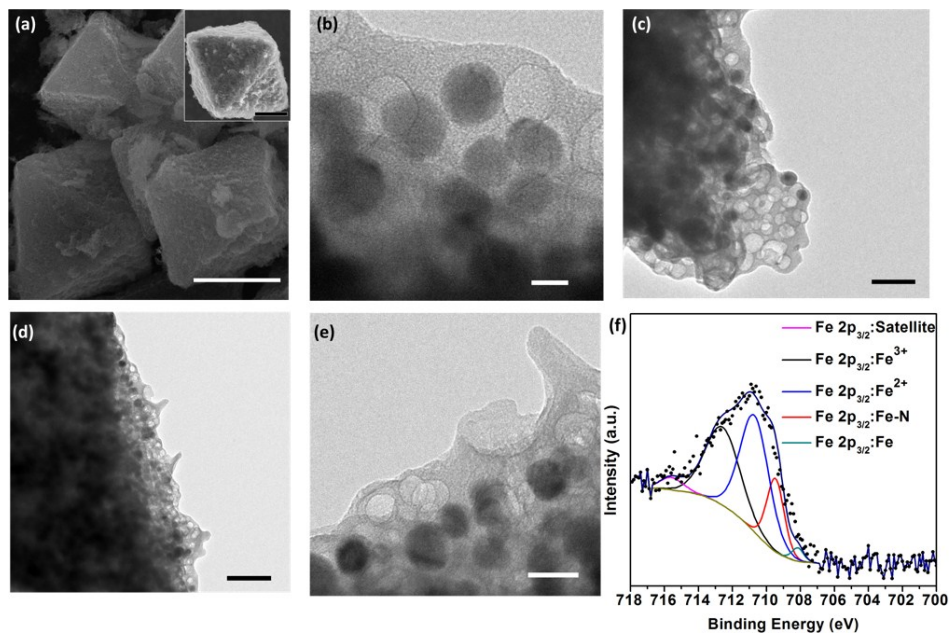


Figure S1 Characterizations of precursors for Fe₂N@NPC. (a) SEM image of the as prepared HKUST-1, scale bar: 2 μm; (b) PXRD patterns of simulated and synthesized HKUST-1;⁹ (c) SEM images of Cu@PC, scale bar: 1 μm, inset: magnified image, scale bar: 500 nm; (d) PXRD pattern of Cu@PC; (e) TEM image (scale bar: 50 nm) and (f) PXRD pattern of PC.



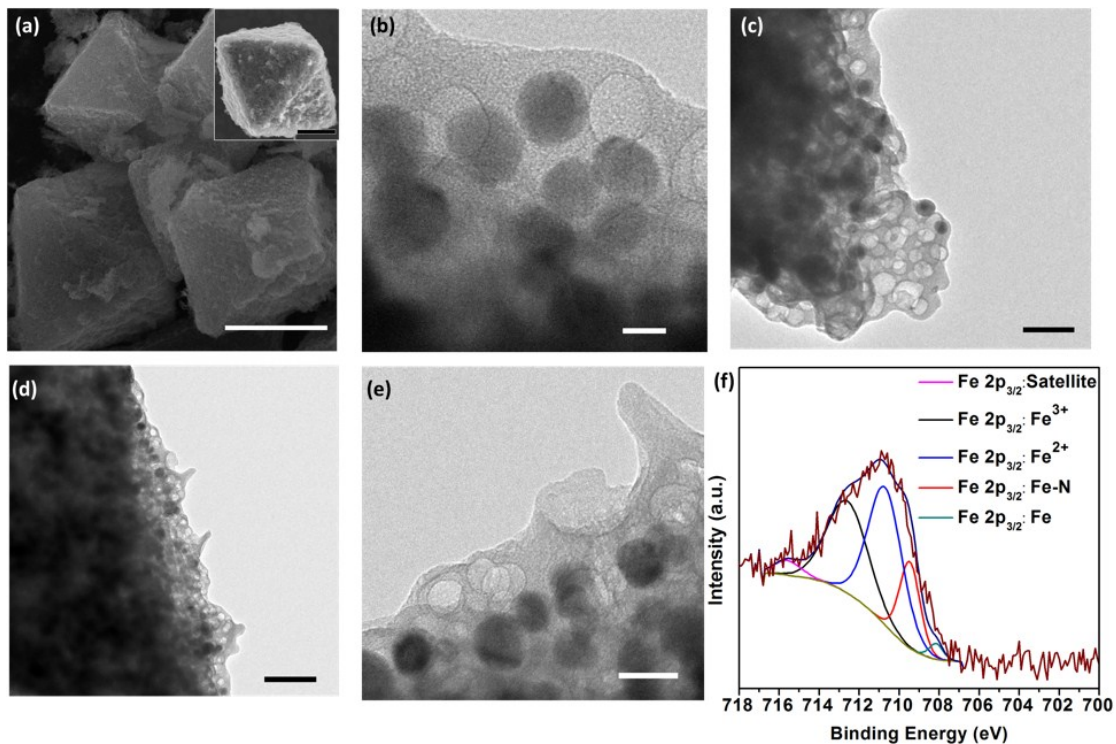


Figure S2 Characterizations of the as prepared $\text{Fe}_2\text{N@NPC-500}$. (a) SEM images of $\text{Fe}_2\text{N@NPC-500}$, scale bar: 3 μm and inset: magnified image, scale bar: 2 μm ; (b) (c) (d) and (e) TEM images of $\text{Fe}_2\text{N@NPC-500}$, scale bar: 20 nm, 50 nm, 500 nm and 50 nm; (f) $\text{Fe } 2p_{3/2}$ high resolution spectrum of $\text{Fe}_2\text{N@NPC-500}$.

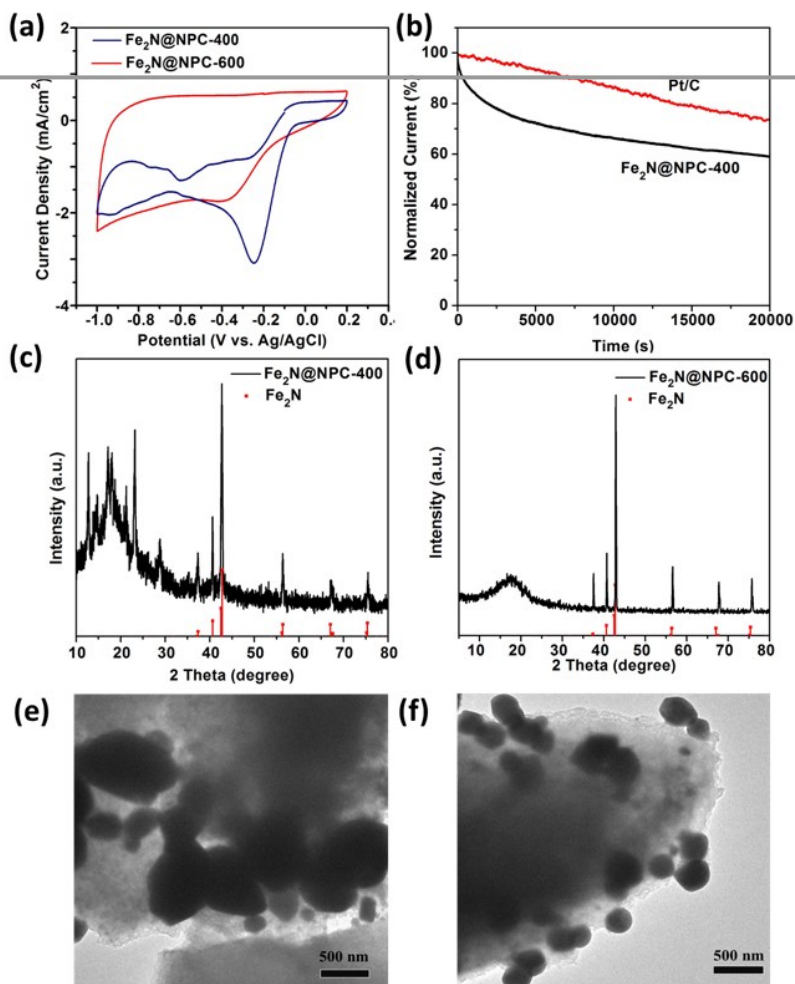


Figure S3 Characterizations of the as prepared Fe₂N@NPC-400 and Fe₂N@NPC-600. (a) CV curves of Fe₂N@NPC-400 and Fe₂N@NPC-600 supported on glassy carbon electrodes in O₂-saturated 0.1 M KOH solution; (b) I-t responses of Fe₂N@NPC-400 and Pt/C at -0.4 V vs Ag/AgCl in O₂-saturated 0.1 M KOH at 400 rpm; (c) and (d) PXRD patterns of the Fe₂N@NPC-400, Fe₂N@NPC-600 and standard XRD pattern PDF#50-0958; (e) and (f) TEM images of Fe₂N@NPC-600, scale bar: 500 nm for e and f.

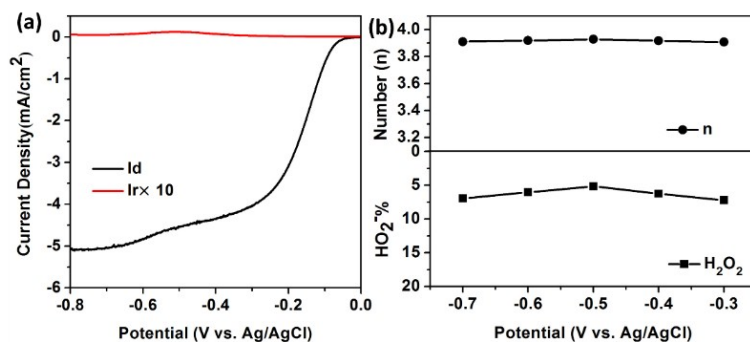


Figure S4 (a) RRDE polarization curves of Fe₂N@NPC-500 in 0.1 M O₂ saturated KOH solution; (b) ORR electron transferred number (n) and yield of H₂O₂ (%) of Fe₂N@NPC-500 based on the corresponding RRDE polarization curves.

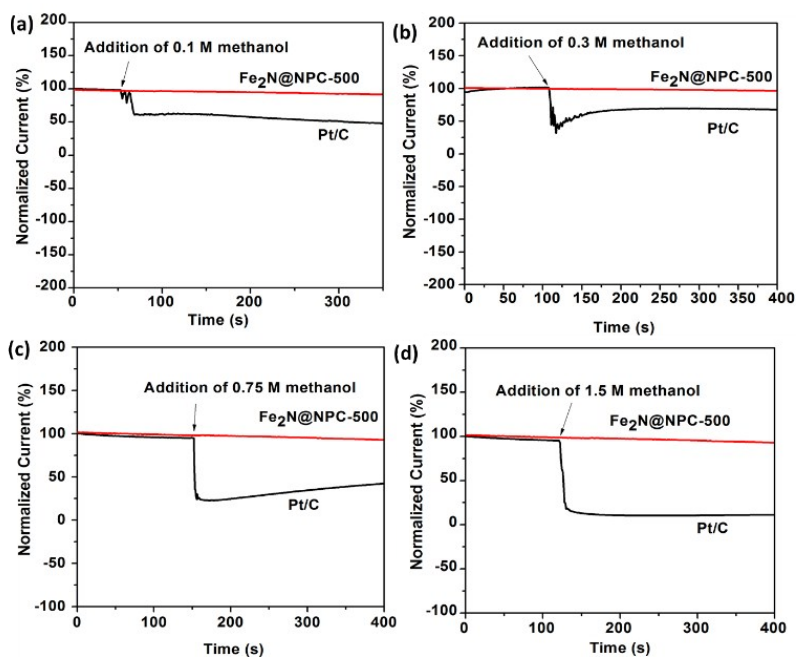


Figure S5 Chronoamperometric responses of Fe₂N@NPC-500 and Pt/C at -0.4 V vs Ag/AgCl in O₂-saturated 0.1 M KOH followed by addition of methanol. (a) for 0.1 M; (b) for 0.3 M; (c) for 0.75M; (d) for 1.5 M,

Various concentration of methanol addition was added to explore the methanol crossover of Fe₂N@NPC-500 and Pt/C. The presence of methanol, even at very low concentration (0.1 M), led to a sharp decrease of current of Pt/C catalysts. Whereas, Fe₂N@NPC-500 showed no obvious change in the current density after the addition of methanol, illustrating a better methanol tolerance than Pt/C in various methanol concentration.

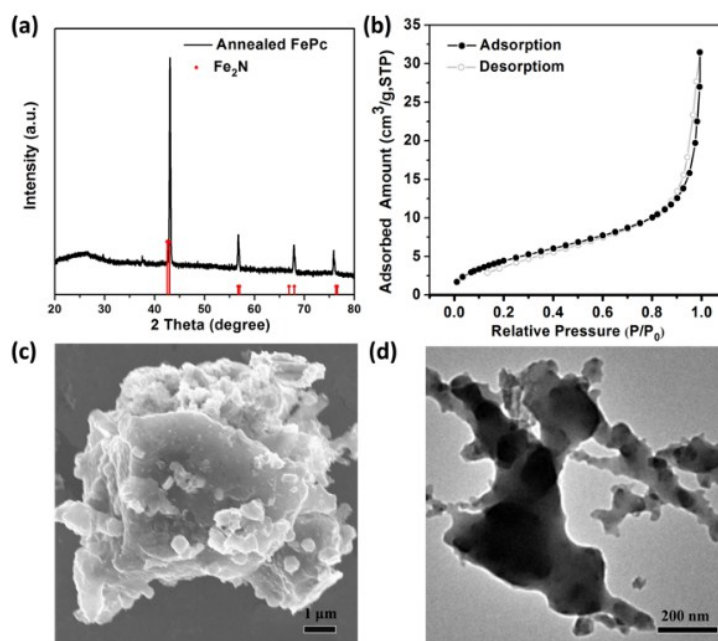


Figure S6 Characterizations of the as-prepared annealed FePc. (a) PXRD pattern of the annealed FePc; (b) Nitrogen sorption and desorption isotherms of the annealed FePc; (c) and (d) SEM and TEM images of the annealed FePc.

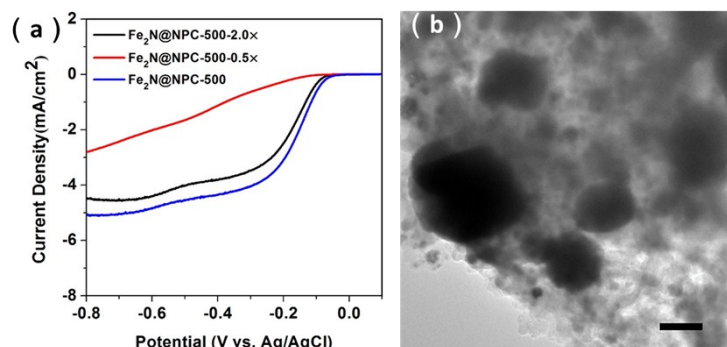


Figure S7 Characterizations of the as-prepared $\text{Fe}_2\text{N@NPC-500-0.5x}$ and $\text{Fe}_2\text{N@NPC-500-2.0x}$. (a) ORR polarization curves of the $\text{Fe}_2\text{N@NPC-500}$, $\text{Fe}_2\text{N@NPC-500-2.0x}$ and $\text{Fe}_2\text{N@NPC-500-0.5x}$ in O_2 -saturated 0.1 M KOH at 1600 rpm; (b) TEM image of the $\text{Fe}_2\text{N@NPC-500-2.0x}$, scale bar: 100 nm

The ORR catalytic performance was evaluated by LSVs of as-prepared $\text{Fe}_2\text{N@NPC}$ catalysts in O_2 saturated 0.1 M KOH solution. In Figure S7a, $\text{Fe}_2\text{N@NPC-500-0.5x}$ showed much lower onset potential and half-wave potential than $\text{Fe}_2\text{N@NPC-500}$, which was due to less incorporation of NPs in $\text{Fe}_2\text{N@NPC-500-0.5x}$ for lower ratio of FePc precursor. Whereas, $\text{Fe}_2\text{N@NPC-500-2.0x}$ also presented slightly lower onset potential, half-wave potential as well as diffusion-limited current density. This might be attributed to the agglomeration of NPs in the NPC caused by excess FePc as shown in TEM image (Figure S7b), which led to lower accessible Fe-N/C active sites capable of ORR catalysis.^{10, 11}

Table S1 BET surface area and pore size distribution of HKUST-1, PC and $\text{Fe}_2\text{N@NPC-500}$.

Samples	BET surface area	Pore size distribution
HKUST-1	1299.5 m^2/g	Micropores
PC	438.5 m^2/g	Micropores, mesopores

Fe ₂ N@NPC-500.	381.4 m ² /g	Micropores, mesopores
----------------------------	-------------------------	-----------------------

Table S2 Element content of NPC, Fe₂N@NPC-500.

Samples	C (wt%)	N (wt%)	O (wt%)	Fe (wt%)
NPC	98.28	1.12	0.59	0.00
Fe ₂ N@NPC-500	96.28	1.89	1.72	0.11

Notes and references

1. K. Okada, R. Ricco, Y. Tokudome, M. J. Styles, A. J. Hill, M. Takahashi and P. Falcaro, *Adv. Funct. Mater.*, 2014, **24**, 1969-1977.
2. I. Kruusenberg, S. Ratso, M. Vikkisk, P. Kanninen, T. Kallio, A. M. Kannan and K. Tammeveski, *J. Power Sources*, 2015, **281**, 94-102.
3. Y. Liang, H. Wang, P. Diao, W. Chang, G. Hong, Y. Li, M. Gong, L. Xie, J. Zhou and J. Wang, *J. Am. Chem. Soc.*, 2012, **134**, 15849-15857.
4. H. Yin, C. Z. Zhang, F. Liu and Y. L. Hou, *Adv. Funct. Mater.*, 2014, **24**, 2930-2937.
5. Y. Liang, Y. Li, H. Wang, J. Zhou, J. Wang, T. Regier and H. Dai, *Nat. Mater.*, 2011, **10**, 780-786.
6. Y. Garsany, O. A. Baturina, K. E. Swider-Lyons and S. S. Kocha, *Analytical Chemistry*, 2010, **82**, 6321-6328.
7. D. van der Vliet, D. S. Strmcnik, C. Wang, V. R. Stamenkovic, N. M. Markovic and M. T. M. Koper, *J. Electroanal. Chem.*, 2012, **666**, 89-89.
8. S. S. Y. Chui, S. M. F. Lo, J. P. H. Charmant, A. G. Orpen and I. D. Williams, *Science*, 1999, **283**, 1148-1150.
9. C. Prestipino, L. Regli, J. G. Vitillo, F. Bonino, A. Damin, C. Lamberti, A. Zecchina, P. L. Solari, K. O. Kongshaug and S. Bordiga, *Chem. Mater.*, 2006, **18**, 1337-1346.
10. J. S. Guo, A. Hsu, D. Chu and R. R. Chen, *J. Phys. Chem. C*, 2010, **114**, 4324-4330.
11. L. Liu, X. Yang, N. Ma, H. Liu, Y. Xia, C. Chen, D. Yang and X. Yao, *Small*, 2016, **12**, 1295-1301.